OMNIX: FROM UNIFIED PANORAMIC GENERATION AND PERCEPTION TO GRAPHICS-READY 3D SCENES

Yukun Huang 1 Jiwen Yu 1,2 Yanning Zhou 3 Jianan Wang 4 Xintao Wang 2 Pengfei Wan 2 Xihui Liu 1†

¹University of Hong Kong ²Kuaishou Technology ³Tencent ⁴Astribot

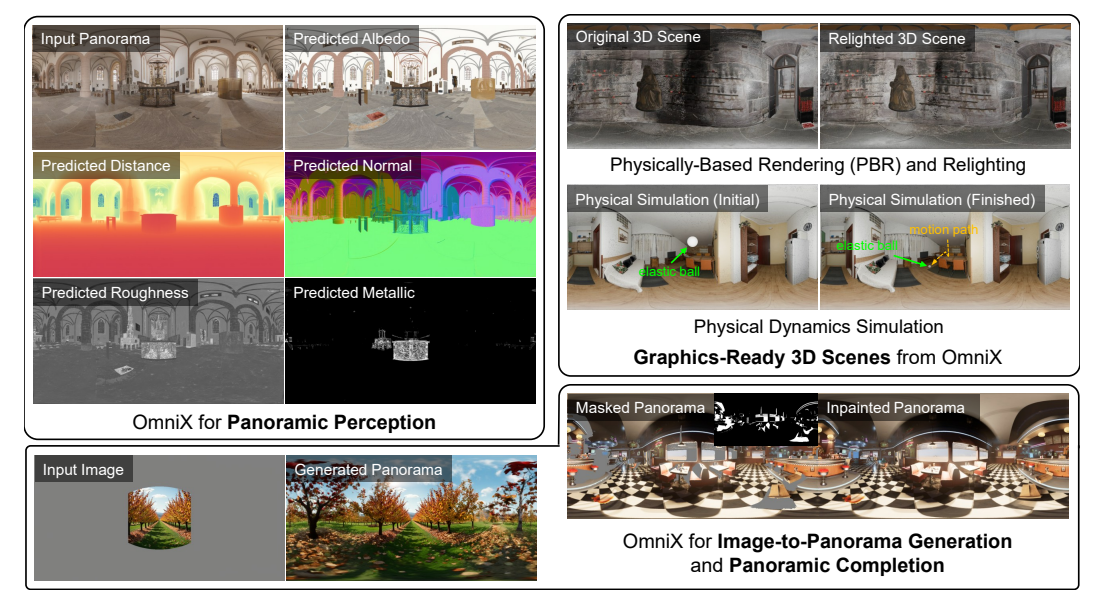


Figure 1: We present **OmniX**, a versatile and unified framework that repurposes pre-trained 2D flow matching models for panoramic perception, generation, and completion. This framework enables the construction of immersive, photorealistic, and graphics-compatible 3D scenes, suitable for physically-based rendering (PBR), relighting, and physical dynamics simulation.

ABSTRACT

There are two prevalent ways to constructing 3D scenes: procedural generation and 2D lifting. Among them, panorama-based 2D lifting has emerged as a promising technique, leveraging powerful 2D generative priors to produce immersive, realistic, and diverse 3D environments. In this work, we advance this technique to generate graphics-ready 3D scenes suitable for physically based rendering (PBR), relighting, and simulation. Our key insight is to repurpose 2D generative models for panoramic perception of geometry, textures, and PBR materials. Unlike existing 2D lifting approaches that emphasize appearance generation and ignore the perception of intrinsic properties, we present OmniX, a versatile and unified framework. Based on a lightweight and efficient cross-modal adapter structure, OmniX reuses 2D generative priors for a broad range of panoramic vision tasks, including panoramic perception, generation, and completion. Furthermore, we construct a large-scale synthetic panorama dataset containing high-quality multimodal panoramas from diverse indoor and outdoor scenes. Extensive experiments demonstrate the effectiveness of our model in panoramic visual perception and graphics-ready 3D scene generation, opening new possibilities for immersive and physically realistic virtual world generation.

[†]Corresponding author.

1 Introduction

Digital replication Dai et al. (2024); Huang et al. (2025b) of 3D scene allows us humans to obtain entertainment and interactive experiences that are difficult to obtain in daily life, or enables near-zero-cost simulation learning for intelligent agents or robots. However, constructing complex 3D scenes requires significant effort and time from artists and engineers, which limits the scale of 3D scene data and hinders the development of native 3D scene generative models.

To automatically build 3D scenes while circumventing data shortages, the community has leveraged large visual language foundation models trained on large-scale text, image, and video data. Based on these powerful models, two typical approaches emerge: procedural generation (Raistrick et al., 2023b;a; Feng et al., 2023) and 2D lifting (Lee et al., 2024; Yu et al., 2024b;c). While procedural generation relies on retrieving objects from a 3D asset library to build the scene, 2D lifting methods directly repurpose 2D generative priors for 3D scene generation, achieving diverse and high-quality results. Recent works (Yang et al., 2025; Huang et al., 2025a; Li et al., 2024b; Zhou et al., 2024) further introduces panoramic representations, which serve as a bridge between 2D and 3D, greatly improving the cross-view consistency of generated 3D scenes. However, these works emphasize appearance generation rather than intrinsic perception, generally using off-the-shelf depth estimation models to extract scene geometry without textures and PBR materials. This hinders the integration of generated 3D scenes into modern graphics pipelines.

In this paper, we introduce **OmniX**, a versatile framework repurposing pre-trained 2D flow matching models for panoramic generation, intrinsic perception, and masked completion. First, we establish a unified formulation for different vision tasks, redirecting the 2D generative paradigm for image-to-panorama generation, panorama-to-X perception, and their generalization with mask guidance. Furthermore, we explore different cross-modal adapter structures capable of handling multiple inputs and propose an effective and flexible adapter structure. This structure can fully reuse 2D generative priors for different vision tasks without significantly changing the pre-trained model weights, effectively improving the performance of panoramic visual perception. In addition, we construct a synthetic panoramic dataset, PanoX, covering indoor and outdoor scenes and various visual modalities such as distance, normal, albedo, roughness, and metallic. This dataset addresses the shortage of high-quality panoramic data with dense geometry and material annotations.

Our main contributions are as follows:

- We present OmniX, a versatile framework repurposing pre-trained 2D flow matching models for panoramic generation, perception, and completion. With a unified formulation and effective cross-modality adapter design, we demonstrate the potential of OmniX to unify panoramic generation, perception, and completion.
- We introduce PanoX, a synthetic panorama dataset encompassing both indoor and outdoor scenes, along with various visual modalities such as depth, normal, albedo, roughness, and metallic maps. This dataset addresses the gap in high-quality panoramic data featuring dense geometry and material annotations.
- Extensive experiments demonstrate the effectiveness of our approach in panoramic perception, generation, and completion. Our method further enables the construction of immersive, photorealistic, and graphics-compatible 3D scenes, ready for PBR rendering, relighting, and physical simulation.

2 RELATED WORK

2.1 INVERSE RENDERING

Inverse rendering (Barrow et al., 1978; Barron & Malik, 2014; Bousseau et al., 2009; Bell et al., 2014; Bhattad et al., 2023; Grosse et al., 2009; Li & Snavely, 2018; Li et al., 2020; Liang et al., 2023; Sengupta et al., 2019; Wang et al., 2021; Wimbauer et al., 2022) aims to estimate intrinsic scene properties such as geometry, materials, and lighting from images. With the rapid progress of generative models, particularly diffusion models, researchers have explored their potential for inverse rendering (Kocsis et al., 2025; Li et al., 2025; Liang et al., 2025; Zeng et al., 2024). In-

trinsiX (Kocsis et al., 2025) generates high-quality PBR maps (albedo, roughness, metallic, normal) from text prompts using a diffusion process, supporting precise material and lighting editing. DiffusionRenderer (Liang et al., 2025) leverages video diffusion models for joint inverse and forward rendering, combining G-buffer estimation with photorealistic image generation through co-training on synthetic and real data.

Panoramic images capture a wider field of view and provide more comprehensive scene information, making them versatile for various applications. Yet, inverse rendering with panoramas remains underexplored. PhyIR (Li et al., 2022) recovers geometry, complex SVBRDFs, and spatially-coherent illumination from a panoramic indoor image using an enhanced SVBRDF model and a physics-based in-network rendering layer to handle complex materials like glossy, metal, and mirror surfaces. However, it is limited to indoor scenes, while we leverage 2D generative priors to generalize across both indoor and outdoor environments.

2.2 3D Scene Generation

Procedural generation (Parish & Müller, 2001; Musgrave et al., 1989; Cordonnier et al., 2017; Raistrick et al., 2023b;a; Yu et al., 2011; Deitke et al., 2022; Feng et al., 2023) automatically creates 3D scenes based on predefined rules or constraints. These methods are scalable and widely used in domains such as gaming, urban planning, and architecture, but often lack diversity and realism due to their rule-based nature. Representative works include CityEngine (Parish & Müller, 2001), which uses grammar-based rules for urban layouts, and Infinigen (Raistrick et al., 2023a), which integrates terrain, material, and creature generators to produce diverse natural environments.

Image- and video-based methods bridge 2D inputs and 3D representations (Dastjerdi et al., 2022; Tang et al., 2023; Lee et al., 2024; Yu et al., 2024a; Li et al., 2024a; Zhang et al., 2024a; Li et al., 2023b; Höllein et al., 2023; Zhang et al., 2024b; Yu et al., 2024d). Image-based approaches reconstruct 3D scenes from single or sequential images using outpainting or depth estimation, with works like ImmerseGAN (Dastjerdi et al., 2022) and MVDiffusion (Tang et al., 2023) generating panoramas for scene synthesis. Video-based methods leverage temporal information to ensure coherent dynamic scenes, exemplified by VividDream (Lee et al., 2024) and 4Real (Yu et al., 2024a). These methods emphasize appearance generation, relying on off-the-shelf depth estimators for geometry while neglecting intrinsic properties such as albedos, normals, and PBR materials.

3 METHOD

3.1 Overview

We introduce OmniX, a versatile framework repurposing pre-trained 2D flow matching models (Esser et al., 2024; Lipman et al., 2023) for panorama perception and generation (Sec. 3.3), which facilitates graphics-ready 3D scene generation (Sec. 3.4). Additionally, we construct a multimodal synthetic panorama dataset, PanoX, which will be introduced in Sec. 3.2.

3.2 PANOX: A MULTIMODAL SYNTHETIC PANORAMA DATASET

Omnidirectional visual perception is crucial for visual understanding and spatial intelligence. To effectively learn perception across a wide field of view (FoV), large-scale panoramic datasets with dense annotations are necessary. While several narrow FoV image datasets (Roberts et al., 2021; Zhu et al., 2022; Li et al., 2023c) offer rich geometry and material annotations, there remains a scarcity of panoramic datasets equipped with dense annotations within the research community.

To this end, we introduce PanoX, a multimodal synthetic panorama Dataset with dense geometry and material annotations. Given the challenges of collecting real panoramic data and the high costs of manual annotation, we leverage synthetic 3D scene assets and the Unreal Engine 5 to generate pixel-aligned multimodal panoramic data. Specifically, our dataset covers 8 large-scale 3D scenes (5 indoor and 3 outdoor scenes) like stores, warehouses, and wilderness. These scenes are rendered into RGB panoramas along with their distance maps, surface normals, albedo, roughness, and metallicity. A preview of PanoX is shown in Figure 2. We also provide text descriptions corresponding to the panoramic images, which are extracted using Florence 2 (Xiao et al., 2024). The

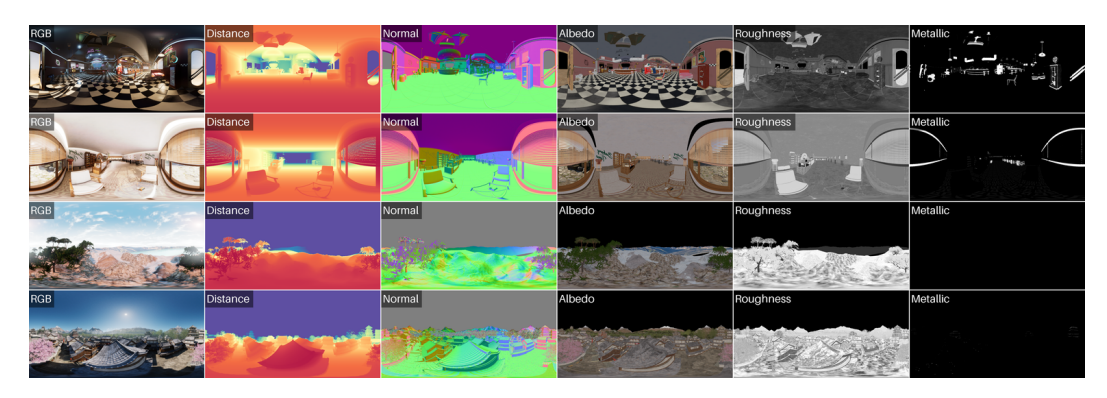


Figure 2: A preview of the proposed PanoX dataset, providing high-quality panoramic rendered images with rich pixel-aligned annotations, including distance, world normal, albedo, roughness, and metallic. The dataset is collected from both indoor and outdoor scenes.

entire dataset contains more than 10,000 instances, corresponding to 60,000 panoramic images of different modalities. We split the six PanoX scenes into training, validation, and test segments in an 8:1:1 ratio, resulting in PanoX-Train, PanoX-Val, and PanoX-Test. The remaining two scenes are grouped as PanoX-OutDomain for generalization evaluation.

We compare the proposed PanoX dataset with existing synthetic scene datasets, as shown in Table 1. To the best of our knowledge, the proposed PanoX is the first panoramic dataset covering both indoor and outdoor scenes with dense geometry and material annotations.

Table 1: Comparison between existing synthetic scene datasets and our proposed PanoX.

Datasets	Geometry Annotation	Material Annotation	Panorama	Indoor	Outdoor
InteriorNet (Li et al., 2018)	✓	✓	√ †	✓	×
Structured3D (Zheng et al., 2020)	\checkmark	×	\checkmark	\checkmark	×
Hypersim (Roberts et al., 2021)	\checkmark	×	×	\checkmark	×
InteriorVerse (Zhu et al., 2022)	\checkmark	\checkmark	×	\checkmark	×
FutureHouse [‡] (Li et al., 2022)	\checkmark	\checkmark	✓	\checkmark	×
MatrixCity (Li et al., 2023c)	\checkmark	\checkmark	×	×	\checkmark
PanoX (Ours)	✓	✓	✓	✓	✓

[†] InteriorNet only contains panoramic RGB images without geometry and material annotations.

3.3 OMNIX: UNIFIED PANORAMIC GENERATION, PERCEPTION, AND COMPLETION

OmniX is a versatile framework for unified panoramic perception and generation, built on the pretrained 2D flow matching model, FLUX.1-dev (Labs, 2025). The overall pipeline is shown in Figure 3. Before delving into the technical details, we first provide a general formulation for unified visual perception and generation.

Unified formulation. Typically, a flow matching-based image generator f_{θ} is trained to predict the velocity vector \mathbf{v} from latent representation \mathbf{z}_0 to latent representation \mathbf{z}_1 , given a textual prompt y and the current timestep t:

$$\mathbf{v}_t = f_{\theta}(\mathbf{z}_t, y, t),\tag{1}$$

The predicted target \hat{z}_1 can be obtained by solving the following ordinary differential equation:

$$\hat{\mathbf{z}}_1 = \mathbf{z}_0 + \int_0^1 \mathbf{v}_t \, dt = \mathbf{z}_0 + \int_0^1 f_\theta(\mathbf{z}_t, y, t) dt.$$
 (2)

Our goal is to expand this image generation paradigm into a unified panoramic generation, perception, and completion framework and serve the subsequent 3D scene construction. To this end, we

[‡] FutureHouse is no longer publicly available.

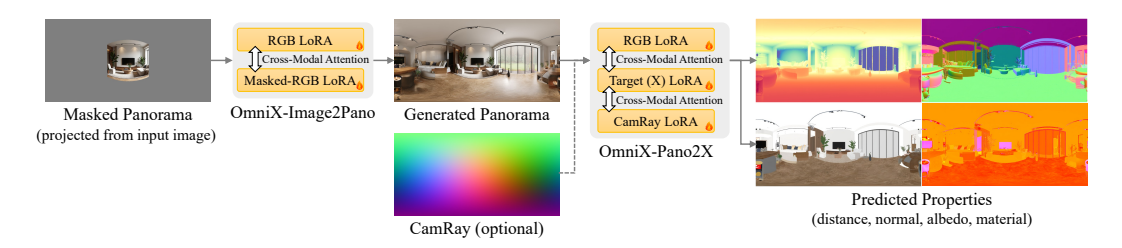


Figure 3: **OmniX** pipeline for panoramic generation and perception. Built on a pre-trained 2D flow matching model with flexible, modality-specific adapters, OmniX is capable of performing a wide range of panoramic vision tasks including generation, perception, and completion.

generalize the model f_{θ} to take multiple condition inputs:

$$\hat{\mathbf{z}}_1 = \mathbf{z}_0 + \int_0^1 f_{\theta}(\mathbf{z}_t, \mathbf{c}^0, \mathbf{c}^1, ..., y, t) dt, \tag{3}$$

where $\{\mathbf{c}^i|i=0,1,...\}$ are the input conditions spatially aligned with \mathbf{z}_t . The modality and number of \mathbf{c}^i depends on the specific task. We explore three task settings throughout this paper:

- (i) For panoramic generation and completion tasks, we define \mathbf{c}^0 as the masked panorama, and \mathbf{c}^1 as the corresponding mask. Specifically, for image-to-panorama generation, the masked panorama is defined as the empty panorama with single-view input image projected onto it.
- (ii) For panoramic perception tasks, *i.e.*, RGB \rightarrow X, we define \mathbf{c}^0 as the RGB reference, and set $y = \emptyset$. The target \mathbf{z}_1 can be any visual modality, such as depth (Euclidean distance for panoramas), normal, albedo, roughness, and metallic. Optionally, additional conditions can be provided to improve performance, for example, further defining \mathbf{c}^1 as a camera ray.
- (iii) For panoramic guided perception tasks, we define \mathbf{c}^0 as the RGB reference, \mathbf{c}^1 as the masked target, and \mathbf{c}^2 as the corresponding mask. The textual prompt y is set to \varnothing . This task setting is necessary for progressive completion when building 3D scenes.

Cross-modal adapter structure. The flexibility of Diffusion Transformer (DiT) (Peebles & Xie, 2023) enables multiple ways to adapt the DiT-based flow matching model for multiple cross-modal 2D inputs, as shown in Figure 4. Specifically, depending on how branches and adapters are shared, these methods can be divided into: Shared-Branch, Shared-Adapter, and Separate-Adapter. Given multiple condition inputs, Shared-Branch and Shared-Adapter are concatenations of channel-wise and token-wise approaches, respectively. Building upon token-wise concatenation, Separate-Adapter assigns different adapters to different types of inputs. Note that different types of input and output share 2D positional encoding since they are spatially-aligned.

In subsequent experiments, we demonstrate that the Separate-Adapter architecture achieves best visual perception performance (Table 4) and allows flexible expansion of inputs and outputs without significantly changing the distribution of model weights.

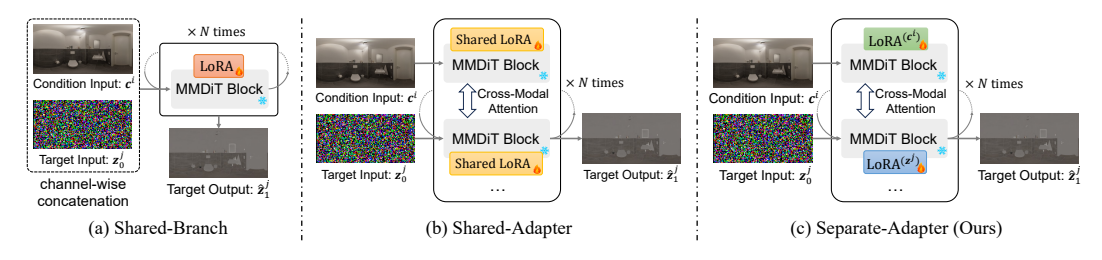


Figure 4: **Different cross-modal adapter structures** for multiple condition inputs $\{\mathbf{c}^i \mid i=0,1,...\}$ and multiple target outputs $\{\hat{\mathbf{z}}_1^j \mid j=0,1,...\}$. Specifically, (a) *Shared-Branch* concatenates different inputs along the channel dimension; (b) *Shared-Adapter* is equivalent to token-wise concatenation; (c) *Separate-Adapter* learns specific adapter weights for each type of input.

Optimization. Based on the Separate-Adapter architecture, multiple LoRAs (Hu et al., 2022) are optimized to leverage a pre-trained 2D flow matching model for feature extraction of condition inputs and velocity vector prediction of target outputs. While both the condition \mathbf{c} and the target \mathbf{z}_t are input to the DiT model, only the prediction of target are used to compute the flow matching loss Lipman et al. (2023):

$$\mathcal{L} = \mathbb{E}_{t, \mathbf{z}_1, \mathbf{z}_0} \| \mathbf{v} - f_{\theta}(\mathbf{z}_t, \mathbf{c}, t) \|^2, \tag{4}$$

where the velocity vector $\mathbf{v} = \mathbf{z}_1 - \mathbf{z}_0$. Note that this objective can be generalized to Multiple condition Inputs $\{\mathbf{c}^i \mid i=0,1,...\}$ and Multiple target Outputs $\{\mathbf{z}_1^j \mid j=0,1,...\}$, yielding a MIMO version of flow matching loss:

$$\mathcal{L}_{\text{mimo}} = \mathbb{E}_{t, \mathbf{z}_1^j, \mathbf{z}_0} \| \mathbf{v} - f_{\theta}(\mathbf{z}_t, \mathbf{c}^0, \mathbf{c}^1, ..., t) \|^2.$$
 (5)

Remarks. Although this paper focuses on panoramic data, the OmniX framework established above can also be applied to narrow FoV images. We try not to introduce inductive bias of omnidirectional representations, thereby preserving the 2D generative priors of the pre-trained model. However, we empirically found that the DiT model has difficulty learning the seam continuity of ERP panoramas, which may be attributed to the topological limitations of the 2D position encoding. To this end, we follow LayerPano3D (Yang et al., 2025) and introduce the horizontal blending technique.

3.4 GRAPHICS-READY 3D SCENE GENERATION

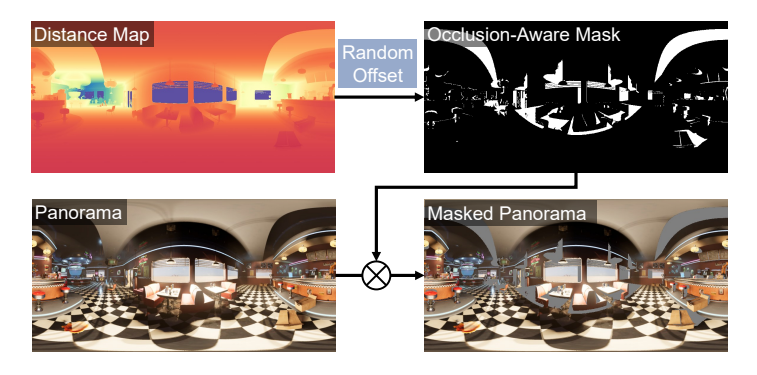
Leveraging the OmniX framework, we are able to construct graphics-ready 3D scenes from a single image input. The entire pipeline consists of three stages: (a) multimodal panorama generation, (b) scene reconstruction, and (c) interactive completion.

Multimodal panorama generation. The proposed OmniX framework offers a general solution for image-to-panorama generation and RGB-to-X panorama perception. We train multiple adapters to repurpose the pre-trained flow matching model for these tasks. Ultimately, by switching adapters of different tasks, we can achieve a generative chain of "image \rightarrow panorama \rightarrow panorama with geometric and intrinsic properties".

Scene reconstruction. Given a panoramic distance map, since the ray direction corresponding to each pixel is known, the pixels can be projected into 3D space as vertices of a 3D mesh, following DreamCube (Huang et al., 2025a). The connectivity of these vertices can be further determined based on pixel neighbors and relative distances. Once the 3D mesh of the scene is obtained, the panoramic maps of other modalities (*i.e.*, albedo, normal, roughness, and metallic) can be assigned to each triangle face via spherical UV unwrapping, resulting in a PBR-ready scene-level 3D asset.

Interactive completion. A single panoramic image is only an omnidirectional observation from a fixed position, so the reconstructed scene does not support free exploration. Interactive scene completion (Yang et al., 2025; Yu et al., 2024b) is important for constructing explorable and even city-scale 3D scenes. To this end, we enhance the OmniX adapters with mask input and fine-tune them for completion and guided perception, resulting in OmniX-Fill. In particular, to simulate scene holes caused by occlusion, we design a depth-based sampling technique to produce occlusion-aware masks, as illustrated in Figure 5. When interactively completing a scene, panoramic completion and guided perception allow generating new regions while preserving existing ones.

Figure 5: Occlusion-aware mask sampling. Based on the panoramic distance map and a randomly sampled 3D displacement, we can estimate the occluded regions by ray intersection. These regions are used as masks for training panoramic completion and guided panoramic perception models.



4 EXPERIMENT

4.1 IMPLEMENTATION DETAIL

We trained 12 adapter models based on Flux.1-dev for different vision tasks, including: OmniX-Image2Pano, OmniX-Pano2Depth, OmniX-Pano2Normal, OmniX-Pano2Albedo, OmniX-Pano2Roughness, OmniX-Pano2Metallic, and their corresponding OmniX-Fill versions. Each of the adapter model consists of two or more LoRAs, depending on the number of inputs and outputs.

Our method is implemented in PyTorch, trained and evaluated on four Ascend 910B NPUs with batch size of 1. All models use the same optimization settings. We adopt an AdamW optimizer with learning rate of 1e-4 for training. No learning rate decay strategy is employed. For graphics-related applications, we develop based on Blender 4.2 and deploy them on an Nvidia L40S GPU.

4.2 EXPERIMENTAL SETUP

Datasets. We utilize the proposed PanoX (Sec. 3.2), Structured3D (Zheng et al., 2020), and HDR360-UHD (Chen et al., 2022) datasets for training and evaluation. The details of PanoX are given in Sec. 3.2. Structured3D (Zheng et al., 2020) is a large-scale photo-realistic dataset, containing about 20,000 indoor panoramas with albedo, depth, normal, and semantic annotations. HDR360-UHD (Chen et al., 2022) is an HDR panorama dataset collected from online resources, covering both indoor and outdoor scenes. We convert these HDR images into LDR images and remove samples with invalid areas, resulting in thousands of high-quality RGB panoramas.

For panoramic perception, we use the standard training splits of both PanoX and Structured3D as training sets. Each training batch is sampled from these two data sources with equal probability. In particular, Structured3D does not include PBR materials, so only PanoX is used when training the roughness and metallic perception models. For panoramic generation, we use the entire HDR360-UHD dataset as the training set, where the text prompts are extracted by BLIP 2 Li et al. (2023a). All panoramic images are resized to a resolution of 512×1024 during training.

Evaluation metrics. For visual perception tasks with ground truths, we adopt a variety of quantitative metrics for different modalities. Specifically, we use PSNR (Peak Signal-to-Noise Ratio) and LPIPS (Zhang et al., 2018) as metrics for albedo, roughness, and metallic. For Euclidean distances, we use four commonly used metrics: AbsRel, δ -1.25, MAE, and RMSE, following the implementation in Cheng et al. (2018). For surface normals, We measure the pixel-wise angular error with ground truth and report the mean, median, and the percentage of pixels with an error below 5° and 30° following Bae & Davison (2024). Note that there may be invalid values in the ground truths (*e.g.*, pixels at infinite distance), we exclude these invalid values when calculating the metrics.

Table 2: **Quantitative evaluation of OmniX on panoramic intrinsic decomposition** compared to five competitors: RGB↔X (Zeng et al., 2024), MGNet (Zhu et al., 2022), IDArb (Li et al., 2025), IID (Kocsis et al., 2024), and DiffusionRenderer (Liang et al., 2025). For fair comparison, we use PanoX-OutDomain as the test set to ensure all methods are evaluated in unseen scenarios.

Methods	Alb	edo	Roug	hness	Metallic		
1110111043	PSNR↑	LPIPS↓	PSNR↑	LPIPS↓	PSNR↑	LPIPS↓	
$RGB \leftrightarrow X$	6.347	0.591	8.175	0.628	4.384	0.720	
MGNet	7.934	0.583	10.219	0.625	6.368	0.656	
IDArb	9.420	0.562	9.572	0.603	4.296	0.554	
IID	10.250	0.640	10.092	0.631	7.891	0.726	
DiffusionRenderer	10.906	0.556	10.445	0.591	14.453	0.425	
OmniX	17.755	0.344	16.211	0.398	18.874	0.254	

4.3 RESULTS ON PANORAMIC PERCEPTION

We divide panoramic perception into intrinsic image decomposition (albedo, roughness, metallic) and geometry estimation (distance, normal), and present both qualitative and quantitative results compared to the state-of-the-art methods.

Panoramic intrinsic decomposition. We compare our OmniX with five state-of-the-art intrinsic decomposition methods: RGB↔X (Zeng et al., 2024), MGNet Zhu et al. (2022), IDArb Li et al. (2025), IID (Kocsis et al., 2024), DiffusionRenderer (Liang et al., 2025). Note that DiffusionRenderer is a video-based inverse rendering method, so we render each panorama into multiple frames to fit its input. The quantitative results are reported in Table 2. Our method achieves consistent state-of-the-art performance on the prediction of three intrinsic properties: albedo, roughness, and metallic. A qualitative comparison is shown in Figure 6 to illustrate the prediction results.

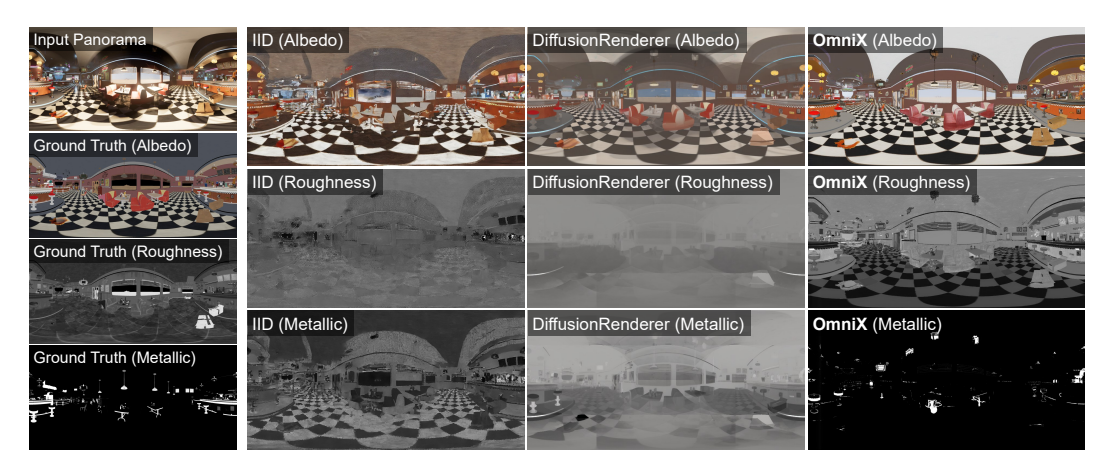


Figure 6: **Qualitative evaluation of OmniX on panoramic intrinsic decomposition** compared to state-of-the-art methods: IID (Kocsis et al., 2024), and DiffusionRenderer (Liang et al., 2025).

Panoramic geometry estimation. We compare our OmniX with two panoramic geometry estimation methods: DepthAnyCamera (Guo et al., 2025), DepthAnywhere Wang & Liu (2024), and four narrow-FoV geometry estimation methods: OmniData-v2 (Kar et al., 2022), MGNet Zhu et al. (2022), DiffusionRenderer (Liang et al., 2025), and MoGe (Wang et al., 2025). The quantitative results are reported in Table 3, where we achieve the highest normal estimation accuracy and and the second highest depth estimation accuracy. Note that MoGe (Wang et al., 2025) integrate 21 large-scale datasets for training, while we use much less data to achieve competitive performance. We further provide a qualitative comparison in Figure 7 to illustrate the prediction results.

Table 3: Quantitative evaluation of OmniX on panoramic geometry estimation compared to state-of-the-art methods: DiffusionRenderer (Liang et al., 2025), MGNet (Zhu et al., 2022), DepthAnywhere (Wang & Liu, 2024), OmniData-v2 (Kar et al., 2022), DepthAnyCamera (Guo et al., 2025), and MoGe (Wang et al., 2025). For fair comparison, we use PanoX-OutDomain as the evaluation set to ensure all methods are evaluated in unseen scenarios.

Methods	Distance				Normal				
1/10/11/0/05	AbsRel↓	δ-1.25↑	MAE↓	RMSE↓	Mean↓	Median↓	5°↑	30°↑	
DiffusionRenderer	0.709	0.246	2.553	16.095	97.186	89.621	0.001	0.023	
MGNet	0.433	0.396	3.972	11.321	79.955	82.836	0.019	0.269	
DepthAnywhere	0.345	0.392	1.804	9.590	/	/	/	/	
OmniData-v2	0.342	0.440	1.944	10.763	85.220	100.596	0.150	0.245	
DepthAnyCamera	0.199	0.680	1.930	7.858	/	/	/	/	
MoGe	0.106	0.898	1.039	5.352	/	/	/	/	
OmniX	0.158	0.787	1.680	6.828	27.138	14.879	0.155	0.663	

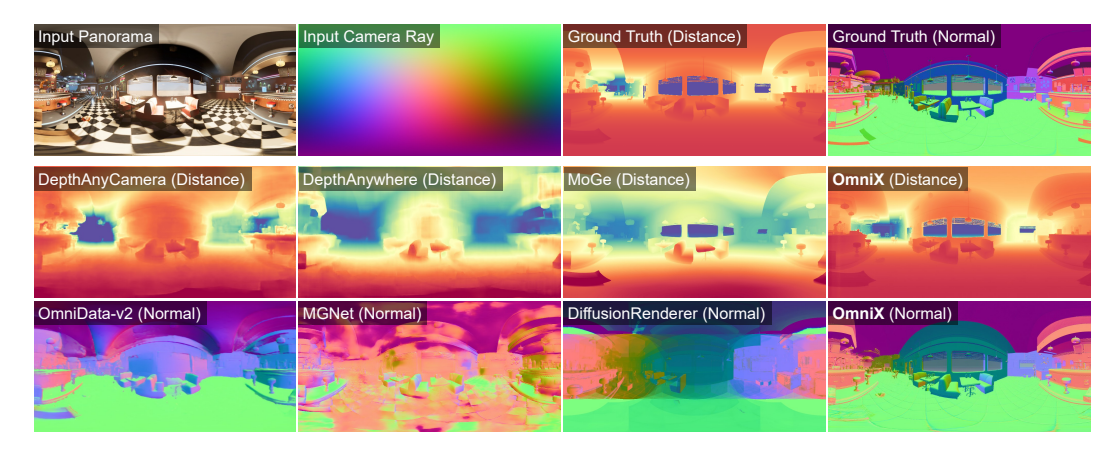


Figure 7: Qualitative evaluation of OmniX on panoramic geometry estimation compared to state-of-the-art geometry estimation methods: DepthAnyCamera (Guo et al., 2025), DepthAnywhere (Wang & Liu, 2024), OmniData-v2 (Kar et al., 2022), MGNet (Zhu et al., 2022), DiffusionRenderer (Liang et al., 2025), and MoGe (Wang et al., 2025). Our approach demonstrates a notable advantage in capturing fine image details, thanks to the proposed cross-modal adapter structure that effectively leverages 2D generative priors to enhance visual perception.

In-the-wild panoramic perception. We empirically find that the proposed OmniX demonstrates superior generalization performance and is able to achieve satisfactory prediction results on in-the-wild images from the Internet. These results are presented in the supplementary material.

4.4 ABLATION ANALYSIS AND DISCUSSION

We explore the impacts of adapter structures and camera rays on panoramic perception performance. Further ablation analysis and discussion are provided in the supplementary material.

Impact of adapter structures. We experimentally analyze the impact of different adapter architectures on panoramic perception performance, as shown in Table 4. The Separate-Adapter structure adopted by OmniX achieved the best performance, thanks to its full reuse of the 2D generative prior for feature extraction of the reference image and prediction of the target modality, without significantly changing the distribution of the pre-trained model weights.

Table 4: **Impact of adapter structures.** We utilize PanoX-Test and PanoX-OutDomain together as the evaluation set to comprehensively cover both in-domain and out-domain scenarios.

Settings	Albedo		Roughness		Distance				
	PSNR↑	LPIPS↓	PSNR↑	LPIPS↓	δ-1.25↑	AbsRel↓	RMSE↓	MAE↓	
Shared-Branch	15.294	0.650	11.729	0.667	0.464	0.386	8.565	2.122	
Shared-Adapter	20.462	0.305	16.920	0.363	0.689	0.219	6.346	1.363	
Separate-Adapter (Ours)	21.682	0.260	18.162	0.329	0.808	0.154	4.755	1.110	

Impact of camera ray inputs. Camera rays are considered important for spatial perception and understanding. We investigate the impact of incorporating camera rays as additional input on visual perception performance. As reported in Table 5, the introduction of camera rays slightly improves the estimation accuracy of normal maps, but has no significant improvement on other modalities.

4.5 APPLICATIONS

OmniX enables automatic production of graphics-ready 3D scenes, as described in Section 3.4. To evaluate the practicality of these generated 3D scenes, we import them into Blender and implement various graphics workflows, including free exploration, PBR-based relighting, and physical simulation. Specifically, for free exploration, we move the camera forward to render a novel panoramic

Table 5: **Impact of camera ray inputs.** We utilize PanoX-Test and PanoX-OutDomain together as the evaluation set to comprehensively cover both in-domain and out-domain scenarios.

Settings	Settings Distance AbsRel \downarrow δ -1.25 \uparrow		Normal		Albedo		Roughness	Metallic
8			Mean↓	Median↓	PSNR↑	LPIPS↓	PSNR↑	PSNR↑
w/o CamRay	0.154	0.808	20.578	11.715	21.682	0.260	18.162	24.643
w/ CamRay	0.155	0.808	19.917	10.992	21.287	0.260	17.590	25.523

view. For PBR-based relighting, we add a point light source and animate its horizontal movement in a circular path around the scene's center. For physical simulation, we introduce an elastic ball into the scene, assigning it an initial horizontal velocity to enable dynamic interactions within the environment. Demonstration videos for these workflows are provided in the project page.

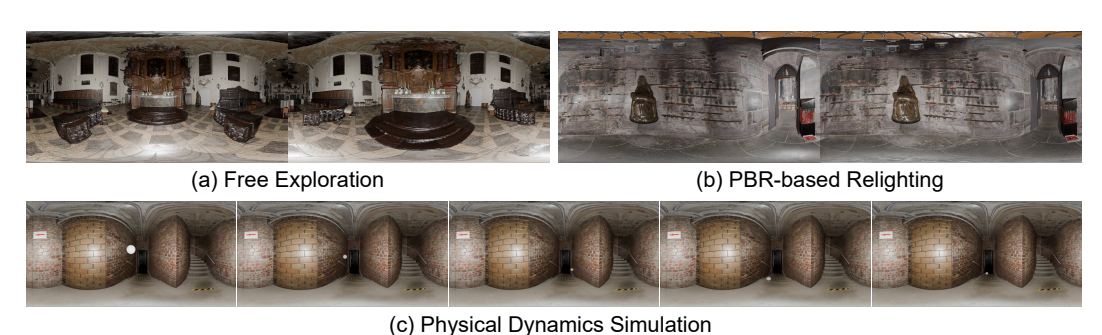


Figure 8: **Demonstrations of the graphics-compatible 3D scenes created with OmniX**, ready for free exploration, PBR-based relighting, and physical dynamics simulation.

5 CONCLUSION

In this work, we present OmniX, a versatile framework for repurposing pre-trained 2D flow matching models for panoramic perception, generation, and completion. Specifically, we establish a unified formulation that incorporates dense visual perception (RGB \rightarrow X) and visual completion (masked X \rightarrow X) into a 2D generative paradigm, and propose an efficient and lightweight cross-modal adapter architecture to model diverse task-specific knowledge. Furthermore, we collect a synthetic panoramic dataset, PanoX, which covers indoor and outdoor scenes and various visual modalities. PanoX provides a panoramic perception benchmark for the community, addressing the shortage of panoramic data with dense geometry and material annotations. Comprehensive experiments validate the effectiveness of our approach in panoramic perception, generation, and completion. Additionally, our method facilitates the creation of immersive, photorealistic, and graphics-compatible 3D scenes, seamlessly integrating with PBR rendering, relighting, and physical simulation workflows.

REFERENCES

- Gwangbin Bae and Andrew J Davison. Rethinking Inductive Biases for Surface Normal Estimation. In *Proceedings of the IEEE/CVF Conference on Computer Vision and Pattern Recognition*, pp. 9535–9545, 2024.
- Jonathan T Barron and Jitendra Malik. Shape, illumination, and reflectance from shading. *IEEE transactions on pattern analysis and machine intelligence*, 37(8):1670–1687, 2014.
- Harry Barrow, J Tenenbaum, A Hanson, and E Riseman. Recovering intrinsic scene characteristics. *Comput. vis. syst*, 2(3-26):2, 1978.
- Sean Bell, Kavita Bala, and Noah Snavely. Intrinsic images in the wild. *ACM Transactions on Graphics (TOG)*, 33(4):1–12, 2014.
- Anand Bhattad, Daniel McKee, Derek Hoiem, and David Forsyth. Stylegan knows normal, depth, albedo, and more. *Advances in Neural Information Processing Systems*, 36:73082–73103, 2023.
- Adrien Bousseau, Sylvain Paris, and Frédo Durand. User-assisted intrinsic images. In *ACM SIG-GRAPH Asia*, pp. 1–10, 2009.
- Zhaoxi Chen, Guangcong Wang, and Ziwei Liu. Text2light: Zero-shot text-driven hdr panorama generation. *ACM Transactions on Graphics (TOG)*, 41(6):1–16, 2022.
- Xinjing Cheng, Peng Wang, and Ruigang Yang. Depth estimation via affinity learned with convolutional spatial propagation network. In *Proceedings of the European conference on computer vision (ECCV)*, pp. 103–119, 2018.
- Guillaume Cordonnier, Eric Galin, James Gain, Bedrich Benes, Eric Guérin, Adrien Peytavie, and Marie-Paule Cani. Authoring landscapes by combining ecosystem and terrain erosion simulation. *ACM Transactions on Graphics (TOG)*, 36(4):1–12, 2017.
- Tianyuan Dai, Josiah Wong, Yunfan Jiang, Chen Wang, Cem Gokmen, Ruohan Zhang, Jiajun Wu, and Li Fei-Fei. Automated creation of digital cousins for robust policy learning. *arXiv preprint arXiv:2410.07408*, 2024.
- Mohammad Reza Karimi Dastjerdi, Yannick Hold-Geoffroy, Jonathan Eisenmann, Siavash Khodadadeh, and Jean-François Lalonde. Guided co-modulated gan for 360 field of view extrapolation. In 2022 International Conference on 3D Vision (3DV), pp. 475–485. IEEE, 2022.
- Matt Deitke, Eli VanderBilt, Alvaro Herrasti, Luca Weihs, Kiana Ehsani, Jordi Salvador, Winson Han, Eric Kolve, Aniruddha Kembhavi, and Roozbeh Mottaghi. Procthor: Large-scale embodied ai using procedural generation. *Advances in Neural Information Processing Systems*, 35:5982–5994, 2022.
- Patrick Esser, Sumith Kulal, Andreas Blattmann, Rahim Entezari, Jonas Müller, Harry Saini, Yam Levi, Dominik Lorenz, Axel Sauer, Frederic Boesel, et al. Scaling Rectified Flow Transformers for High-Resolution Image Synthesis. In *International Conference on Learning Representations*, 2024.
- Weixi Feng, Wanrong Zhu, Tsu-jui Fu, Varun Jampani, Arjun Akula, Xuehai He, Sugato Basu, Xin Eric Wang, and William Yang Wang. Layoutgpt: Compositional visual planning and generation with large language models. *Advances in Neural Information Processing Systems*, 36: 18225–18250, 2023.
- Roger Grosse, Micah K Johnson, Edward H Adelson, and William T Freeman. Ground truth dataset and baseline evaluations for intrinsic image algorithms. In 2009 IEEE 12th International Conference on Computer Vision, pp. 2335–2342. IEEE, 2009.
- Yuliang Guo, Sparsh Garg, S Mahdi H Miangoleh, Xinyu Huang, and Liu Ren. Depth Any Camera: Zero-Shot Metric Depth Estimation from Any Camera. In *Proceedings of the Computer Vision and Pattern Recognition Conference*, pp. 26996–27006, 2025.

- Lukas Höllein, Ang Cao, Andrew Owens, Justin Johnson, and Matthias Nießner. Text2room: Extracting textured 3d meshes from 2d text-to-image models. In *Proceedings of the IEEE/CVF International Conference on Computer Vision*, pp. 7909–7920, 2023.
- Edward J Hu, Yelong Shen, Phillip Wallis, Zeyuan Allen-Zhu, Yuanzhi Li, Shean Wang, Lu Wang, Weizhu Chen, et al. LoRA: Low-Rank Adaptation of Large Language Models. In *International Conference on Learning Representations*, 2022.
- Yukun Huang, Yanning Zhou, Jianan Wang, Kaiyi Huang, and Xihui Liu. DreamCube: 3D Panorama Generation via Multi-plane Synchronization. *arXiv preprint arXiv:2506.17206*, 2025a.
- Zhening Huang, Xiaoyang Wu, Fangcheng Zhong, Hengshuang Zhao, Matthias Nießner, and Joan Lasenby. Litereality: Graphics-ready 3d scene reconstruction from rgb-d scans. *arXiv preprint arXiv:2507.02861*, 2025b.
- Oğuzhan Fatih Kar, Teresa Yeo, Andrei Atanov, and Amir Zamir. 3d common corruptions and data augmentation. In *Proceedings of the IEEE/CVF Conference on Computer Vision and Pattern Recognition*, pp. 18963–18974, 2022.
- Peter Kocsis, Vincent Sitzmann, and Matthias Nießner. Intrinsic Image Diffusion for Indoor Singleview Material Estimation. In *Proceedings of the IEEE/CVF Conference on Computer Vision and Pattern Recognition*, pp. 5198–5208, 2024.
- Peter Kocsis, Lukas Höllein, and Matthias Nießner. IntrinsiX: High-Quality PBR Generation using Image Priors. In *Advances in Neural Information Processing Systems*, 2025.
- Black Forest Labs. Flux.1-dev. https://huggingface.co/black-forest-labs/FLUX.1-dev, 2025. Accessed: 2025-01-19.
- Yao-Chih Lee, Yi-Ting Chen, Andrew Wang, Ting-Hsuan Liao, Brandon Y Feng, and Jia-Bin Huang. Vividdream: Generating 3d scene with ambient dynamics. *arXiv preprint arXiv:2405.20334*, 2024.
- Junnan Li, Dongxu Li, Silvio Savarese, and Steven Hoi. Blip-2: Bootstrapping language-image pre-training with frozen image encoders and large language models. In *International conference on machine learning*, pp. 19730–19742. PMLR, 2023a.
- Renjie Li, Panwang Pan, Bangbang Yang, Dejia Xu, Shijie Zhou, Xuanyang Zhang, Zeming Li, Achuta Kadambi, Zhangyang Wang, Zhengzhong Tu, et al. 4k4dgen: Panoramic 4d generation at 4k resolution. *arXiv preprint arXiv:2406.13527*, 2024a.
- Wenbin Li, Sajad Saeedi, John McCormac, Ronald Clark, Dimos Tzoumanikas, Qing Ye, Yuzhong Huang, Rui Tang, and Stefan Leutenegger. InteriorNet: Mega-scale Multi-sensor Photo-realistic Indoor Scenes Dataset. In *British Machine Vision Conference (BMVC)*, 2018.
- Wenrui Li, Fucheng Cai, Yapeng Mi, Zhe Yang, Wangmeng Zuo, Xingtao Wang, and Xiaopeng Fan. SceneDreamer360: Text-Driven 3D-Consistent Scene Generation with Panoramic Gaussian Splatting. *arXiv preprint arXiv:2408.13711*, 2024b.
- Xingyi Li, Zhiguo Cao, Huiqiang Sun, Jianming Zhang, Ke Xian, and Guosheng Lin. 3d cinemagraphy from a single image. In *Proceedings of the IEEE/CVF Conference on Computer Vision and Pattern Recognition*, pp. 4595–4605, 2023b.
- Yixuan Li, Lihan Jiang, Linning Xu, Yuanbo Xiangli, Zhenzhi Wang, Dahua Lin, and Bo Dai. MatrixCity: A Large-scale City Dataset for City-scale Neural Rendering and Beyond. In *Proceedings of the IEEE/CVF International Conference on Computer Vision*, pp. 3205–3215, 2023c.
- Zhen Li, Lingli Wang, Xiang Huang, Cihui Pan, and Jiaqi Yang. PhylR: Physics-Based Inverse Rendering for Panoramic Indoor Images. In *Proceedings of the IEEE/CVF Conference on Computer Vision and Pattern Recognition*, pp. 12713–12723, 2022.
- Zhengqi Li and Noah Snavely. Cgintrinsics: Better intrinsic image decomposition through physically-based rendering. In *Proceedings of the European conference on computer vision (ECCV)*, pp. 371–387, 2018.

- Zhengqin Li, Mohammad Shafiei, Ravi Ramamoorthi, Kalyan Sunkavalli, and Manmohan Chandraker. Inverse rendering for complex indoor scenes: Shape, spatially-varying lighting and svbrdf from a single image. In *Proceedings of the IEEE/CVF conference on computer vision and pattern recognition*, pp. 2475–2484, 2020.
- Zhibing Li, Tong Wu, Jing Tan, Mengchen Zhang, Jiaqi Wang, and Dahua Lin. IDArb: Intrinsic Decomposition for Arbitrary Number of Input Views and Illuminations. In *International Conference on Learning Representations*, 2025.
- Ruofan Liang, Huiting Chen, Chunlin Li, Fan Chen, Selvakumar Panneer, and Nandita Vijaykumar. Envidr: Implicit differentiable renderer with neural environment lighting. In *Proceedings of the IEEE/CVF International Conference on Computer Vision*, pp. 79–89, 2023.
- Ruofan Liang, Zan Gojcic, Huan Ling, Jacob Munkberg, Jon Hasselgren, Chih-Hao Lin, Jun Gao, Alexander Keller, Nandita Vijaykumar, Sanja Fidler, et al. Diffusion Renderer: Neural Inverse and Forward Rendering with Video Diffusion Models. In *Proceedings of the Computer Vision and Pattern Recognition Conference*, pp. 26069–26080, 2025.
- Yaron Lipman, Ricky TQ Chen, Heli Ben-Hamu, Maximilian Nickel, and Matthew Le. Flow Matching for Generative Modeling. In *International Conference on Learning Representations*, 2023.
- F Kenton Musgrave, Craig E Kolb, and Robert S Mace. The synthesis and rendering of eroded fractal terrains. *ACM Siggraph Computer Graphics*, 23(3):41–50, 1989.
- Yoav IH Parish and Pascal Müller. Procedural modeling of cities. In *Proceedings of the 28th annual conference on Computer graphics and interactive techniques*, pp. 301–308, 2001.
- William Peebles and Saining Xie. Scalable Diffusion Models with Transformers. In *Proceedings of the IEEE/CVF international conference on computer vision*, pp. 4195–4205, 2023.
- Alexander Raistrick, Lahav Lipson, Zeyu Ma, Lingjie Mei, Mingzhe Wang, Yiming Zuo, Karhan Kayan, Hongyu Wen, Beining Han, Yihan Wang, et al. Infinite photorealistic worlds using procedural generation. In *Proceedings of the IEEE/CVF conference on computer vision and pattern recognition*, pp. 12630–12641, 2023a.
- Alexander Raistrick, Lahav Lipson, Zeyu Ma, Lingjie Mei, Mingzhe Wang, Yiming Zuo, Karhan Kayan, Hongyu Wen, Beining Han, Yihan Wang, et al. Infinite photorealistic worlds using procedural generation. In *Proceedings of the IEEE/CVF conference on computer vision and pattern recognition*, pp. 12630–12641, 2023b.
- Mike Roberts, Jason Ramapuram, Anurag Ranjan, Atulit Kumar, Miguel Angel Bautista, Nathan Paczan, Russ Webb, and Joshua M. Susskind. Hypersim: A Photorealistic Synthetic Dataset for Holistic Indoor Scene Understanding. In *Proceedings of the IEEE/CVF International Conference on Computer Vision*, pp. 10912–10922, 2021.
- Soumyadip Sengupta, Jinwei Gu, Kihwan Kim, Guilin Liu, David W Jacobs, and Jan Kautz. Neural inverse rendering of an indoor scene from a single image. In *Proceedings of the IEEE/CVF International Conference on Computer Vision*, pp. 8598–8607, 2019.
- Shitao Tang, Fuyang Zhang, Jiacheng Chen, Peng Wang, and Yasutaka Furukawa. MVDiffusion: Enabling Holistic Multi-view Image Generation with Correspondence-Aware Diffusion. In *Advances in Neural Information Processing Systems*, 2023.
- Ning-Hsu Albert Wang and Yu-Lun Liu. Depth Anywhere: Enhancing 360 Monocular Depth Estimation via Perspective Distillation and Unlabeled Data Augmentation. *Advances in Neural Information Processing Systems*, 37:127739–127764, 2024.
- Ruicheng Wang, Sicheng Xu, Cassie Dai, Jianfeng Xiang, Yu Deng, Xin Tong, and Jiaolong Yang. MoGe: Unlocking Accurate Monocular Geometry Estimation for Open-Domain Images with Optimal Training Supervision. In *Proceedings of the Computer Vision and Pattern Recognition Conference*, pp. 5261–5271, 2025.

- Zian Wang, Jonah Philion, Sanja Fidler, and Jan Kautz. Learning indoor inverse rendering with 3d spatially-varying lighting. In *Proceedings of the IEEE/CVF International Conference on Computer Vision*, pp. 12538–12547, 2021.
- Felix Wimbauer, Shangzhe Wu, and Christian Rupprecht. De-rendering 3d objects in the wild. In *Proceedings of the IEEE/CVF Conference on Computer Vision and Pattern Recognition*, pp. 18490–18499, 2022.
- Bin Xiao, Haiping Wu, Weijian Xu, Xiyang Dai, Houdong Hu, Yumao Lu, Michael Zeng, Ce Liu, and Lu Yuan. Florence-2: Advancing a unified representation for a variety of vision tasks. In *Proceedings of the IEEE/CVF Conference on Computer Vision and Pattern Recognition*, pp. 4818–4829, 2024.
- Shuai Yang, Jing Tan, Mengchen Zhang, Tong Wu, Gordon Wetzstein, Ziwei Liu, and Dahua Lin. LayerPano3D: Layered 3D Panorama for Hyper-Immersive Scene Generation. In *SIGGRAPH*, pp. 1–10, 2025.
- Heng Yu, Chaoyang Wang, Peiye Zhuang, Willi Menapace, Aliaksandr Siarohin, Junli Cao, László Jeni, Sergey Tulyakov, and Hsin-Ying Lee. 4real: Towards photorealistic 4d scene generation via video diffusion models. *Advances in Neural Information Processing Systems*, 37:45256–45280, 2024a.
- Hong-Xing Yu, Haoyi Duan, Charles Herrmann, William T Freeman, and Jiajun Wu. Wonderworld: Interactive 3d scene generation from a single image. *arXiv* preprint arXiv:2406.09394, 2024b.
- Hong-Xing Yu, Haoyi Duan, Junhwa Hur, Kyle Sargent, Michael Rubinstein, William T Freeman, Forrester Cole, Deqing Sun, Noah Snavely, Jiajun Wu, et al. Wonderjourney: Going from anywhere to everywhere. In *Proceedings of the IEEE/CVF Conference on Computer Vision and Pattern Recognition*, pp. 6658–6667, 2024c.
- Hong-Xing Yu, Haoyi Duan, Junhwa Hur, Kyle Sargent, Michael Rubinstein, William T Freeman, Forrester Cole, Deqing Sun, Noah Snavely, Jiajun Wu, et al. Wonderjourney: Going from anywhere to everywhere. In *Proceedings of the IEEE/CVF Conference on Computer Vision and Pattern Recognition*, pp. 6658–6667, 2024d.
- Lap-Fai Yu, Sai Kit Yeung, Chi-Keung Tang, Demetri Terzopoulos, Tony F Chan, and Stanley J Osher. Make it home: automatic optimization of furniture arrangement. *ACM Trans. Graph.*, 30 (4):86, 2011.
- Zheng Zeng, Valentin Deschaintre, Iliyan Georgiev, Yannick Hold-Geoffroy, Yiwei Hu, Fujun Luan, Ling-Qi Yan, and Miloš Hašan. RGB↔X: Image Decomposition and Synthesis Using Material-and Lighting-aware Diffusion Models. In *ACM SIGGRAPH*, 2024.
- Cheng Zhang, Qianyi Wu, Camilo Cruz Gambardella, Xiaoshui Huang, Dinh Phung, Wanli Ouyang, and Jianfei Cai. Taming stable diffusion for text to 360 panorama image generation. In *Proceedings of the IEEE/CVF Conference on Computer Vision and Pattern Recognition*, pp. 6347–6357, 2024a.
- Jingbo Zhang, Xiaoyu Li, Ziyu Wan, Can Wang, and Jing Liao. Text2nerf: Text-driven 3d scene generation with neural radiance fields. *IEEE Transactions on Visualization and Computer Graphics*, 30(12):7749–7762, 2024b.
- Richard Zhang, Phillip Isola, Alexei A Efros, Eli Shechtman, and Oliver Wang. The unreasonable effectiveness of deep features as a perceptual metric. In *Proceedings of the IEEE/CVF Conference on Computer Vision and Pattern Recognition*, 2018.
- Jia Zheng, Junfei Zhang, Jing Li, Rui Tang, Shenghua Gao, and Zihan Zhou. Structured 3D: A Large Photo-Realistic Dataset for Structured 3D Modeling. In *Computer Vision–ECCV 2020: 16th European Conference, Glasgow, UK, August 23–28, 2020, Proceedings, Part IX 16*, pp. 519–535. Springer, 2020.

Shijie Zhou, Zhiwen Fan, Dejia Xu, Haoran Chang, Pradyumna Chari, Tejas Bharadwaj, Suya You, Zhangyang Wang, and Achuta Kadambi. Dreamscene360: Unconstrained text-to-3d scene generation with panoramic gaussian splatting. In *European Conference on Computer Vision*, pp. 324–342. Springer, 2024.

Jingsen Zhu, Fujun Luan, Yuchi Huo, Zihao Lin, Zhihua Zhong, Dianbing Xi, Rui Wang, Hujun Bao, Jiaxiang Zheng, and Rui Tang. Learning-Based Inverse Rendering of Complex Indoor Scenes with Differentiable Monte Carlo Raytracing. In *ACM SIGGRAPH Asia*, 2022.

A IN-THE-WILD PANORAMIC PERCEPTION

We provide the panoramic perception results of OmniX on in-the-wild images from the Internet, as shown in Figure 9. Our method demonstrates excellent generalization performance for unseen images. This is due to our proposed adapter architecture effectively reusing the generative priors from pre-trained 2D flow matching model.

B RESULTS ON PANORAMIC GENERATION

We provide the panoramic generation results of OmniX from single-view image inputs, as shown in Figure 10. Our method is able to achieve high-quality and diverse image-to-panorama generation.

C RESULTS ON PANORAMIC COMPLETION

We provide the panoramic completion and guided panoramic perception results of OmniX from masked inputs and corresponding masks, as shown in Figure 11. Our method is able to achieve accurate and locally coherent completion and guided perception for panoramas.

D More Ablation Analysis and Discussion

Impact of joint material modeling. VAEs for 2D latent flow matching models are trained on three-channel RGB inputs, and single-channel PBR material maps cannot be directly processed by the model. As a result, existing methods Kocsis et al. (2024; 2025) concatenate roughness and metallic together with an additional 0-channel for three-channel input. We explore the impact of different PBR material input arrangements on visual perception performance, as shown in Table 6. We find that that directly concatenating PBR material maps in the channel dimension is suboptimal, resulting in poor performance and blurred prediction results. A better practice is to jointly model PBR materials in a cross-attention manner.

Table 6: **Impact of joint PBR material modeling.** We utilize PanoX-Test and PanoX-OutDomain together as the evaluation set to comprehensively cover both in-domain and out-domain scenarios.

Settings	Roug	hness	Met	allic	Average		
	PSNR↑	LPIPS↓	PSNR↑	LPIPS↓	PSNR↑	LPIPS↓	
joint (concat.)	17.660	0.350	24.575	0.323	21.118	0.337	
joint (cross-attn.)	17.427	0.340	25.425	0.138	21.426	0.239	
independent	18.162	0.329	24.643	0.153	21.403	0.241	

Impact of joint geometry modeling. Euclidean distance maps and normal maps are strongly correlated, so intuitively modeling them jointly should lead to improved performance. However, as shown in Table 7, such joint geometry modeling does not bring positive performance gains for the prediction of either modality. This may be because the model fails to learn the geometric relationship between distance and normal vectors from the limited training data.

Table 7: **Impact of joint geometry modeling.** We utilize PanoX-Test and PanoX-OutDomain together as the evaluation set to comprehensively cover both in-domain and out-domain scenarios.

Settings		Dista	ınce	Normal				
	AbsRel↓	δ-1.25↑	MAE↓	RMSE↓	Mean↓	Median↓	5°↑	30°↑
joint (cross-attn.)	0.163	0.787	1.113	5.348	20.800	11.950	0.227	0.767
independent	0.155	0.808	1.084	5.347	19.917	10.992	0.249	0.779

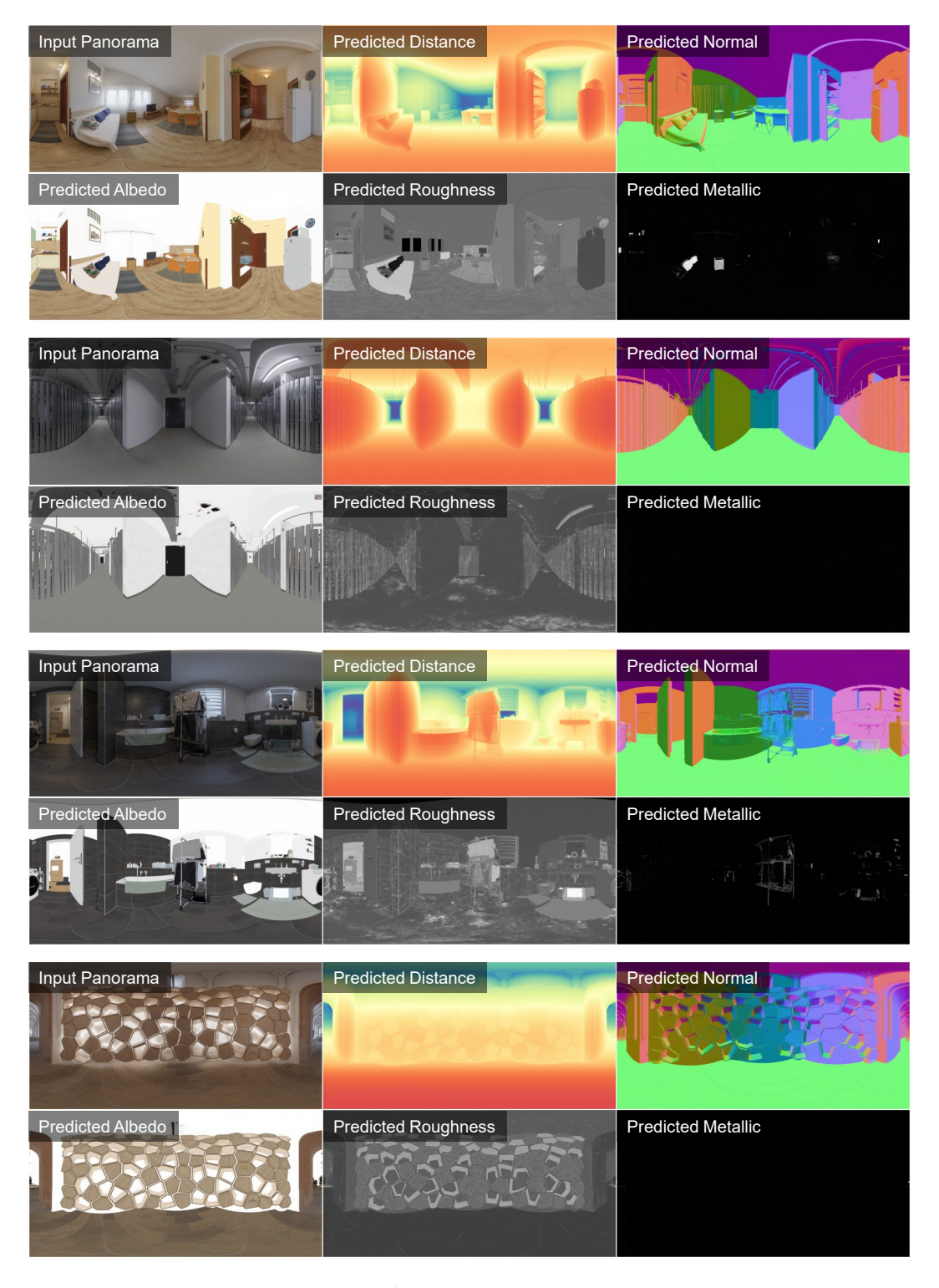


Figure 9: Panoramic perception results of OmniX on in-the-wild images. Our method demonstrates excellent generalization performance on unseen images.

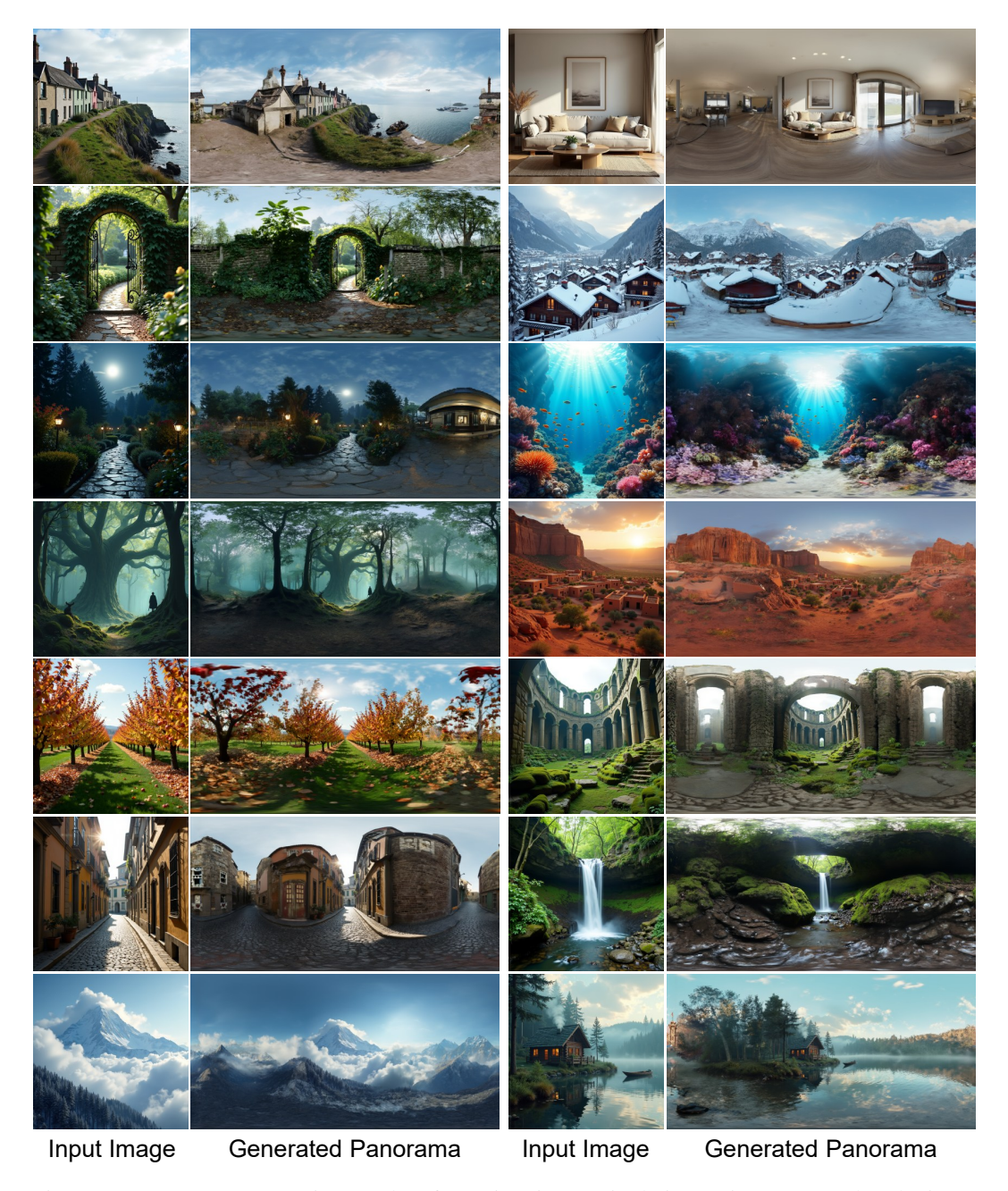


Figure 10: Panorama generation results of OmniX given a single image input. Note that the input single-view image is generated by Flux.1-dev (Labs, 2025).

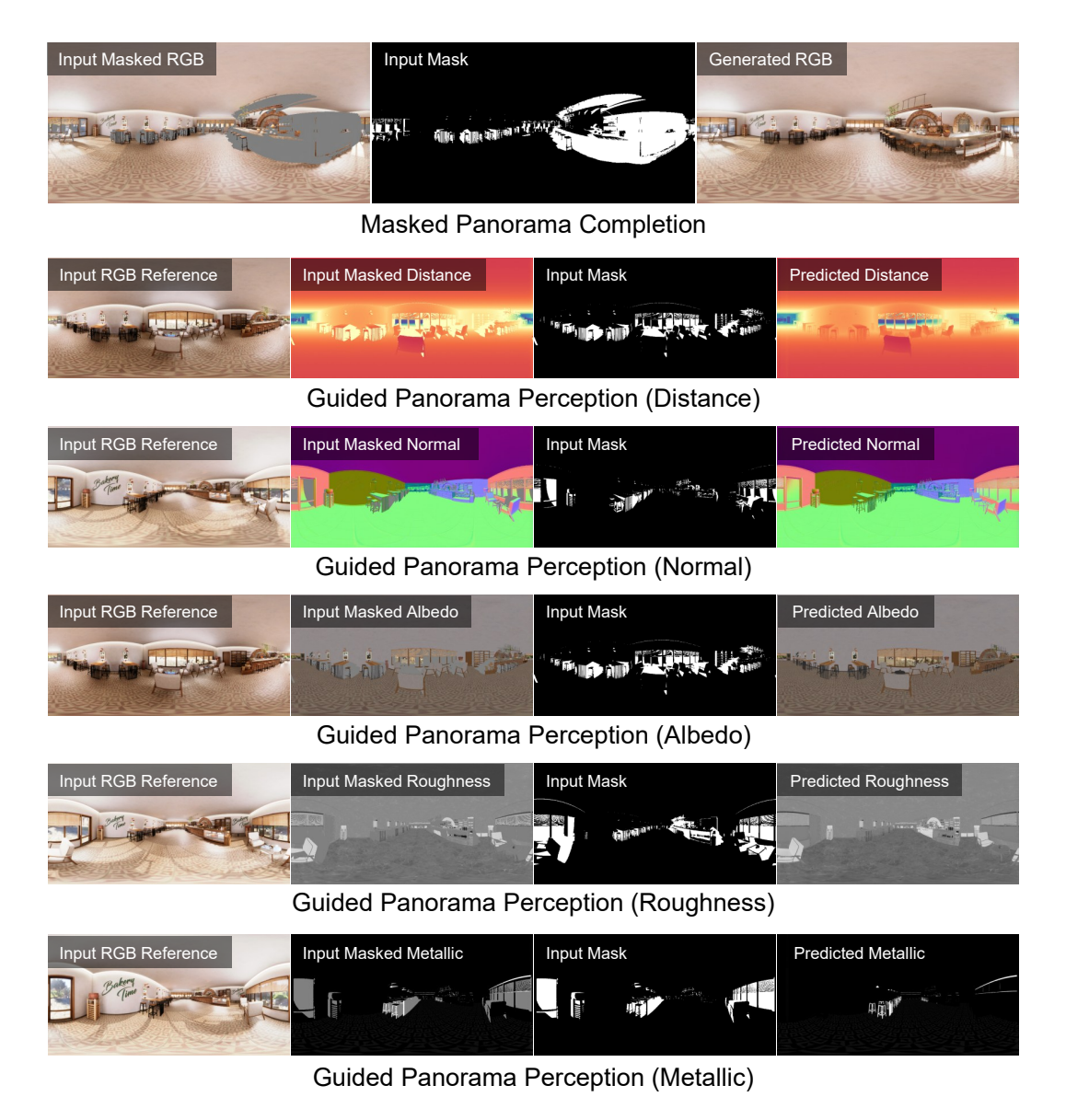


Figure 11: Panorama completion and guided panoramic perception results of OmniX. Given masked inputs and corresponding masks, OmniX is able to generate accurate and locally coherent results for masked areas. For guided panoramic perception, extra RGB references are input to ensure that the prediction results are consistent with RGB references.

E LIMITATIONS

Our method is built on top of pre-trained 2D flow matching models and thus inherits their shortcomings such as slow training and inference efficiency. In addition, OmniX's prediction of Euclidean distance is still not accurate enough, resulting in bumpy reconstructed 3D surfaces, which affects the subsequent PBR rendering effect. We also empirically observe that OmniX-Pano2Metallic, used for metallic prediction, performs poorly in generalization. This is partly due to the scarcity of panoramic PBR material data for training. Furthermore, the significant differences between neural rendering (*i.e.*, 2D generative modeling) and PBR rendering may indicate that pre-trained 2D image priors have limited benefits for PBR material estimation.